Int. J. Econ. Environ. Geol. Vol. 13 (3) 15-21, 2022
Journal home page: www.econ-environ-geol.org
Open Access
ISSN: 2223-957X

Polymer Stabilized Metal Nanoparticles for Catalytic Degradation of Methylene Blue in Water

Mohsin Khadam[1], Habib Ullah[2*], Saif Ullah[1], M. Athar Faheem Riaz[1], Hamza Khan Lodhi[1]

[1]Department of Chemistry, University of Lahore, Lahore, Punjab, Pakistan
[2]Department of Chemistry, Lahore Garrison University, Punjab, Pakistan

* Email: habibullah6728@gmail.com

Received: *13 May, 2022* ***Accepted:*** *26 June, 2022*

Abstract: Methylene blue is highly toxic and releases from various industries. It must be transformed into less toxic compounds. The Core-Shell microgels p (Pst core), Pstcore-NIPMamm-MAa and Ag in Pst-p NIPMamm-MAa have been synthesized using the Core-Shell hybrid micro gelling NIPMamm-MAa emulsion polymerization process. The 0.086mM, MB 6.2mM NaBH4 and 0.2916 mg / mL catalysts in the cuvette were measured using UV-visible spectrophotometers. Spectrums were measured at a one-minute interval. The peak at 600 nm steadily decreased over time and was completely eliminated after 11 minutes. Without the catalyst, MB decreases with NaBH4 which showed that the reaction decreases were slow and MB very high within 120 minutes. The Psty core of FT-IR core microgels, pNIpmam-MMAA, and Ag-pNIpmam-MAA core microgels are hybrids. At 2955 and 2845 cm^{-1} FT-IR spectra, Psty NiPMaM – MaA and Ag-p NiPMaM – MaA were used for core shell microgels, with C-H vibrations expanding the aromatic ring. In this study degradation of Methylene were carried out with Ag- Nanocomposites at different interval of time to check the degradation at minimum time. The degradation of MB dye were carried out with Ag- Nano composites at different interval of time to check the degradation at minimum time.

Keywords: Methylene blue; Pst core NIPMamm-MAa; Ag-p NiPMaM – MaA; $NaBH_4$; nanoparticles degradation.

Introduction

Nanotechnology sector is one of the most important areas of research and development (Paul and Robeson, 2008). Nano composites carbon-black elastomer enhancements, colloidal silica adjustments and even natural fiber enhancement topics have also been studied for decades. Organic and inorganic Nano composites based on sol-gel chemistry, which have been studied for several decades, are almost lost in the current Nano composite discussions (Mark, 1984; Wen, 1996). The research area of Plasmonics is emerging nowadays for the synthesis and characterization of nanostructures that are very important in this field. The Plasmonics nature of some nanostructures having some versatile applications like biological and chemical sensing and solar energy etc. (Odom and Schatz, 2011). For the preparation of silver nanoparticles and Plasmon nanostructures on photo catalytic systems, light irradiation and dispersion agent techniques have been investigated (Choi et al., 2010). Plasmonics is an advantageous technology that disrupts the large gap between electronic and photonic components. It also provides more circuit sizes reductions and energy efficiency improvements. Plasmonics is based on the stimulation of Surface Plasmon Polaritons (SPP) which are electromagnetic waves bound to free electron oscillations in metals and spread at near-light speed along the metal-dielectric interface (Atwater, 2007; Barnes et al., 2003; Brongersma and Shalaev, 2010). For many years it has been known that metal salts were photo reduced to metal nanoparticles using ketyl radicals. Polymeric matrix as well as photo reducing agent are responsible for nanoparticle distribution, size and shape (Kazancioglu et al., 2021). The main objective of present study is to degrade Methylene blue, which an organic pollutant presents in water resources using Pst core NIPMamm-MAa and Ag-p NiPMaM – MaA.

Materials and Methods

Various substances of their percentage purity used to prepare homogeneous microgels. Microgels of core / shell and composite microgels of core / shell are discussed. There have also been studies of various analytical techniques used to classify prepared microgel samples.
Apparatus used for the synthesis of p Nipmam-Maa microgels, pStycore and pSty-p NIipmam-Maa core/shell microgels and Ag embedded pSty-pNipmam-Maa core/shell hybrid microgels are Three-necked round bottom flask, Condenser, Hot plat, Thermometer, and Teflon stirrer.

Compounds used for synsthesis of p Nipmam-Maa microgels, pStycore and pSty-p NIipmam-Maa core/shell microgels and Ag embedded pSty-pNipmam-Maa core/shell hybrid microgels are, N, N-methylenebisacrylamide (99%), Styrene (98%), Methylene Blue (98%), Methacrylic acid (98%), N-isopropyl methacrylamide (98%), Sodium dodecyl sulfate (98%), Ammonium per sulfate (99%), Sodium hydroxide, Hydrochloric acid, Sodium borohydride (98%), Dialyzing membrane(12,000 to 14,000 cutoff) and Silver nitrate (97%)

Sigma Aldrich, Germany and Gemistone Chemicals have acquired both chemicals. Stand Maa have been

washed using alumina (Al_2O_3) as an adsorber through vacuum filtration to remove the inhibitor (Table 1). Before further purification, all other chemicals were used (Table 2). The dialytic membrane with a pore size of 12000 to 14000 cut off obtained from Fischer research, UK was purged from pure and hybrid microgel suspensions. As previously mentioned, p(NiPMam-Maa) microgels have been manufactured using emulsion polymerization methods such as Nipmam (monomer), SDS (surfactant), M-BIS (cross linker) and APS (initiator). In the 3 neck flasks with condenser and nitrogen gas for up to 12 minutes, 0.69 g (5.7 ml) Nipmam, 0.00281 g (0.179 mmol) MBIS, 0.029 g (0.41 mmol) SDS MAa and 0.013 g SDS were mixed in 43 ml of deionized water. Heating was then initiated and the temperature of the reaction mixture raised by 72° C. After 28 minutes of temperature monitoring at 72 ° C, a 0.076 M solution of 4.5 mL was introduced to the reaction mixture. After a few minutes of addition of APs, the clear mixture was switched on, signaling the start of polymerization. The reaction was continued for 4.5 hours in order to finish the polymerization process under heating, and continuous nitrogen supply. Treatment of 12,000 to 14,000 molecular porous membrane cut-off for 6 days with regular exchange of deionized water filtered the formed microgel particles.

Two step methods including simple emulsion poly merization and seed mediated emulsion poly merization pSty-pNipmam-Maa core / shell microgel have also been created. Initially, 80 mL of water was applied to the three necked bottom flasks with 0.19 g NIPMam, 0.047 g SDS and 1.69 g (1.81 mL). The mixture supplied with nitrogen was stirring for 10 minutes. Heating has started and a temperature of about 70° C has been sustained for 40 minutes. Drop wise was added to the reaction mixture with 9.5 mL (0.068 M) APs. For 6.5 hours, the reaction was continued prepared core PSt latex was dialyzed using porous molecular membrane to eliminate unreacted membranes. In the second level, core latex PST was used for the preparation of pNipmam-Maashell microgels around it. To this end, Maa was blended in the round bottom flask with 55mL deionized water 1,25 g Nipmam, 0,046 g MBIS, 0,046 g SDS, 0,0289 g (28,6µL) Maa and 29mL of pSty core Latex, which were stirring for 8 minutes with nitrogen. The action mixture temperature was held at approximately 75° C. After 35 minutes of temperature maintenance and constant stirring, the mixture added 2 mL of APS solution (0.077 M) and the reaction continued for 4.2 hours. Prepared core / shell microgels of pSty-p (Nip Mam-Maa) have been added slowly to eliminate reactive molecules such as M-BIS, Nipmam Maa, SDS and APS. The core / shell of Ag hybrid microgels at pSty-pNipmam-Maa in situ was prepared using $AgNO_3$ salt as a forerunner to silver nanoparticles and $NaBH_4$ as a reduced ambient temperature (20° C) ingredient following the above technique. 5.7 mL PST-pNipmam-Maa microgel dispersion was applied to 26 ml deionized water (84 percent diluted) taken in three necked round bottom flasks and stirred under nitrogen supply for 12 minutes. The stirrer was added to the $AgNO_3$ salt (0.098 M) water solution in the diluted microgel dispersion for 28 minutes. The reaction mixture was then added to 4.7 mL with freshly made $NaBH_4$ solution (0.047 M) and mixed for another 60 min under the nitrogen supply. Ag was changed to a light brown appearance on the suspension of the core / shell hybrid microgels at pSty-pNipmam-Maa when $NaBH_4$ was applied, which indicates the formation of Ag NP in the polymer network. The core / shell microgel composite suspension was dialyzed at room temperature for half an hour with a 2-time deionized water interchange.

Results and Discussion

Degradation of Methylene blue

Methylene blue was degradd using optimum condition by adding Metal Nanoparticles catalyst and character-ized using UV visible spectrophotometer (Fig. 4.1).

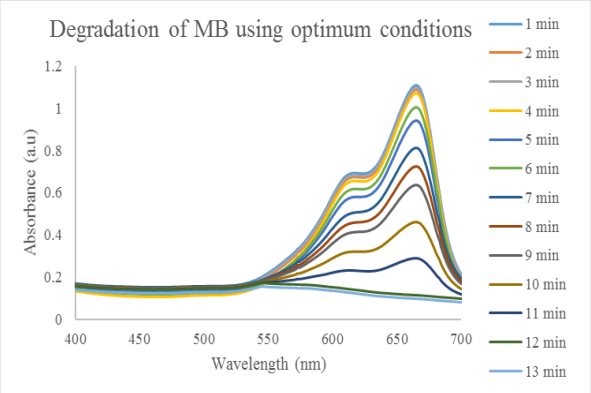

Fig 4.1 Degradation of Methylene blue using optimum conditions; Methylene blue = 0.086mM, $NaBH_4$ = 6.2 mM, Ag-pSty-pNipmam-Maa= 0.2916 mg/mL, Temperature = 34°C.

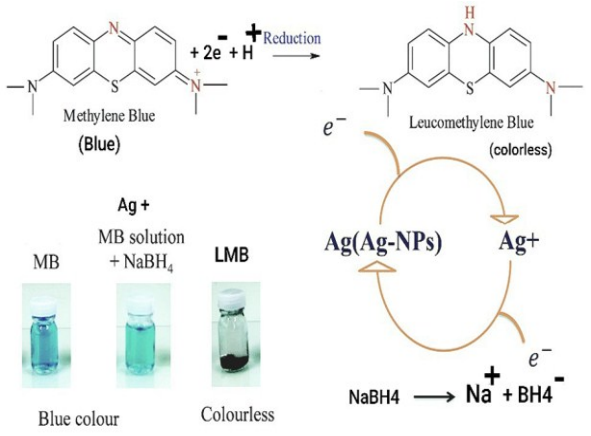

Fig. 4.2 Mechanism of degradation of Methylene blue dye using Ag-PSty-PNiPMaM-MaA-CS catalyst.

In Figure 4.2 Methylene blue acts as substrate reduced by using $NaBH_4$. $NaBH_4$ oxidized itself and give $2e^-$ to break the double bond between nitrogen and carbon which produced leucomethylene blue which is colorless. The nanoparticles absorb at the surface of

methylene blue. Nano-Ag-pSty-pNipmam-Maa was degraded at a suitable temperature with $NaBH_4$ as a reducing agent. Driven experiments were also performed one-by-one in the presence of micro-core shells, composite micro particles and $NaBH_4$. Since the ionization of the COOH groups of polymer chains at pH > pka of Maa, the positive charge of MB molecules are adsorbed on the surface of the nanoparticles and decrease property is enhanced by the fact that the metal nanoparticles and the micro shell are normally negatively charged in the Nano-Ag-pSty-pNipmam-Maa catalyst (Singh et al., 2013). Characterization of the degradation of methylene blue is performed using UV visible spectrophotometry at ideal conditions as shown in graph-4 above using Beer-Lambert Law. A popular and functional expression of the Beer-Lambert Law concerns the optical attenuation by samples and absorption of the species of physical material that contains a single, uniformly attenuating species. This is the mathematical form:

$$\mathbf{A = \varepsilon \ell c}$$

Where,

(ε) is the attenuating species molar attenuation or absorption coefficient
(ℓ) is the path length
(c) is the attenuating species concentration

In Figure 4.1 wavelength (nm) is taken at x-axis and absorbance at y-axis at different interval of time. The range of wavelength selected is 400-700 nm. At different time laps as shown in graph 1, the absorbance at optimum conditions between 1 to 11th minute the reaction goes on. While at 12th and 13th minutes the reaction becomes linear indicating there is no further reactant left.

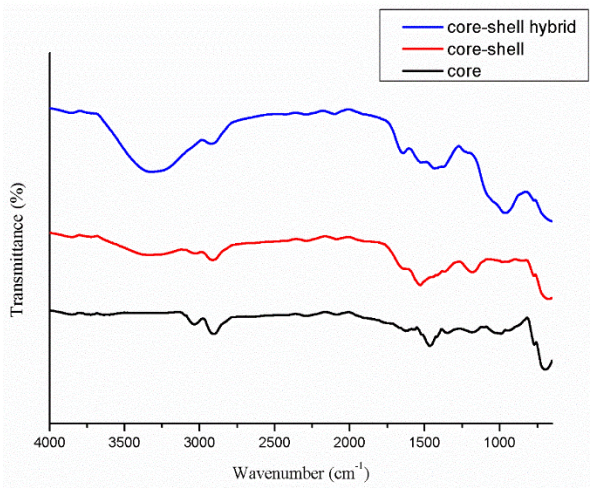

Fig. 4.3 IR spectra of Core, Core-shell and Core-shell hybrid compounds.

Table 3 IR- Interpretation of Core Shell Hybrid compound.

Sr. No.	Dips	Functional Group
1	3300 cm^{-1} (Strongly Broad Dip)	Amide – Stretch
2	2850 cm^{-1}	Alkane – Stretch
3	1630 cm^{-1}	(C=O)- Stretch
4	1465 cm^{-1} (Fingerprint region)	-CH_2- (Bend)

Table 4 IR- Interpretation of Core-Shell compound.

Sr. No.	Dips	Functional Group
1	2850 cm^{-1}	Alkane – Stretch
2	1640 cm^{-1}	(C=O) – Stretch
3	1510 cm^{-1}	C=C (Aromatic)
4	1300 cm^{-1} (Fingerprint region)	C-O

Table 5 IR- Interpretation of Core compound.

Sr. No.	Dips	Functional Group
1	2850 cm^{-1}	Alkane – Stretch
2	3150 cm^{-1}	Aromatic - Stretch (o.o.p)
3	1465 cm^{-1} (Fingerprint region)	C=C (Aromatic)

Figure 4.3 shows FT-IR core microgels of pSty core, pNipmam-Maa and Ag-pSty-pNipmam-Maa heart shell hybrid microgels. From figure it is concluded that hybrid core shell have excellent impact as compared to core shell and core. It means that there are such changes occur in the shape of the core and core shell mircrogels which leads towards the important application for Methylene blue degradation. Such spectrums endorse the encapsulation of the shell region around the PSTY core and core shell hybrid microgels, C-H spectrum of aromatic ring motion, were allocated to 2955 and 2845 cm−1 in FT-IR spectra, pSty-pNipmam-Maa and Ag-pSty-pNipmam-Maa bands (Table 3). Popularity occurs at 3300 cm−1 in the core shell of the pSty-pNipmam-Maa hybrid due to amide-component bonding N to the Nipmam. The peaks at 1630 and 1640cm−1 were observed for both pure and composite microgels as presented in Table 4. The peak was never seen for C = C at 1600 cm−1 from both pure and composite FT-IR microgel spectra indicating polymerization points and the change in C = C to C-C due to vibrations of the Nipmam and Maa monomer groups. The peaks of 1507 and 1456 cm−1 observed in pSty-pNipmam-Maa and Ag-pSty-pNipmam-Maa, the core composite shell microgels were due to C = C bonding in the aromatic ring as presented in Table 5 (Zhu et al., 2008).

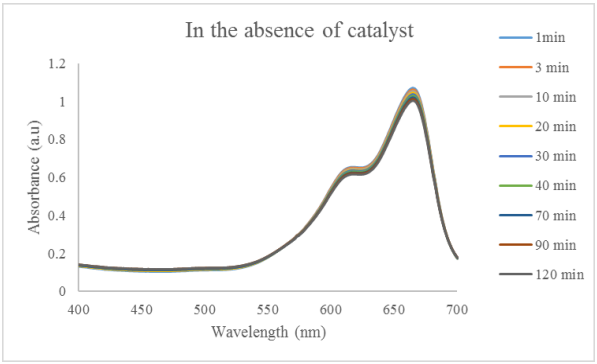

Fig. 4.4 Degradation of blue Methylene in the absence of a catalyst.

In the Absence of Catalyst

Degradation of the MB does not occur in the absence of a catalyst. There is no chance of a reaction. A small decrease of the absorbance at 665 nm after 13 minutes. In the absence of the catalyst, even the colour of the dye does not stay invariant at the end of a day, which indicates that the reduction is very sluggish and

negligible in the absence of the catalyst. The reaction is only conducted in the presence of the nano-catalyst under certain conditions, and then the spectra appear. The reduction rate is maximum and the absorbance is become low and then end in the time of 8 minutes. The color of the mixture also become fads and finally disappear. The reaction stop in 8 minutes shows that the reaction is of high quality in the availability of silver nanoparticles as a catalyst. Time-dependent UV spectra minimize the degradation of MB by the presence of nanoparticle catalysts and composites. The above findings suggest that the absorbance value is reduced by the degradation of MB Control over the surface of Ag NPs due to the loading of composite nanoparticles.

Confirmation of Ag-NPs

This line increase in absorbance is due to presence of light in the visible region. Figure 4.5 shows the confirmation of Ag-NPs while showing the peak at 400 nm. which is a fix wavelength for Ag-NPs. Peak in grey color in Figure 4.5 confirms the presence of Ag-NPs as a catalyst using in the reaction. While peak in blue shows the presence of microgel (P-styrene).

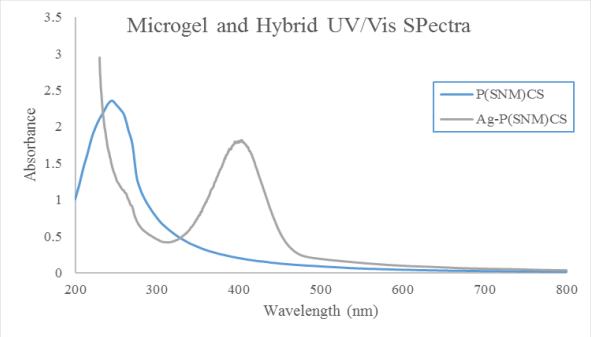

Fig. 4.5. Graph showing the presence of Ag-NPs in the reaction.

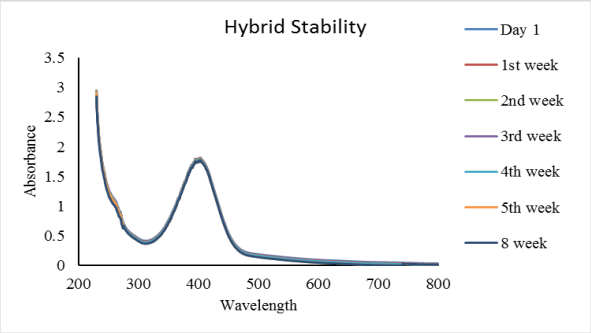

Fig. 4.6: Showing the Stability of Hybrid (Ag-NPs).

Hybrid (Ag-NPs) Stability

In above graph taken wavelength (200 to 800nm) on x-axis and absorbance on y-axis (0.5 to 3.5). Figure 4.6 above shows that the hybrid Nano catalyst-containing microgels are very stable from the beginning and no instability was recorded on the last day during the entire working period. The device shows the same absorbance, maximum 400 nm per week from day 1 to 8. Stability refers to the validation of sample analyses at various time intervals. Here is a graph in Figure 4.6 showing days and weeks. The length of the procedure is 8 weeks. The study was analyzed week by week for up to 8 weeks. The graph demonstrates the stability of the peaks from day one to 8 of the week. The graph shows how stable sample is prepared.

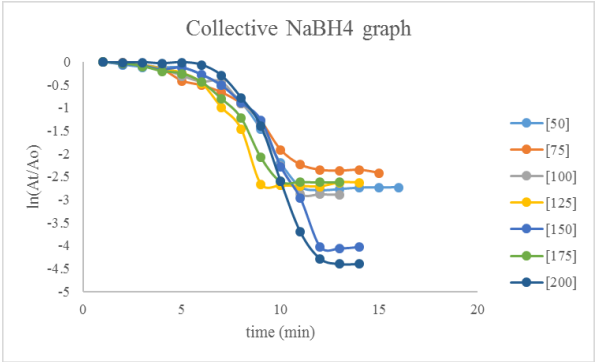

Fig. 4.7 Showing the effect of reducing agent on Ag-pSty-pNipmam-Maa in different time intervals.

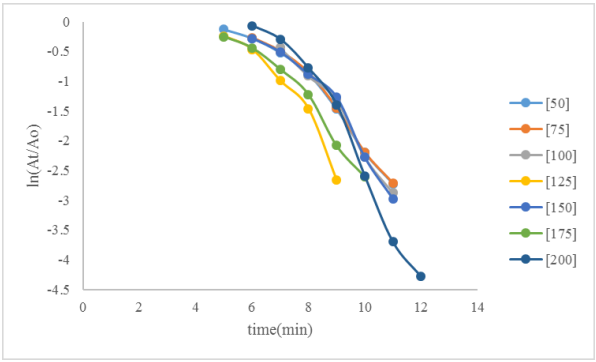

Fig. 4.8 Showing the effect of reducing agent on Ag-pSty-pNipmam-Maa.

Effect of Reducing Agent

At a one-minute interval, UV-visible spectra were scanned. Following the completion of the reaction mixture solution, the Methylene blue was made colorless. In the absence of the catalyst, a reduction in MB with $NaBH_4$ was also carried out as shown in (Fig. 4.8). The decreasing reaction was slow and the MB in 120 minutes was very high. Although the thermodynamically positive reduction of $NaBH_4$ and MB, it is kinetically disadvantageous because of a larger energy boundary between electron donor and accepter in the exclusion of a catalyst (Ajmal et al., 2013). Ag Nps really eliminate the energy barrier and act as an electron relay, for reducing MB acts simultaneously as an electron donor and acceptor. Ag Nps play a major role in electron transfer from BH_4^{-1} to MB (Pradhan et al., 2002). In Figure 4.8 a collective graph was taken containing different peaks showing the effect of reducing agent ($NaBH_4$) at different concentration i.e. 50, 75, 100, 125, 150, 175, and 200 mg/mL. Concentration above and below 125 mg/ml has taken more time to reduce the sample. While the concentration of 125mg/ml showing the best result for reducing of reaction by $NaBH_4$. The reason is that when concentration was below 125mg/ml, the reducing

agent will not cover the maximum sites of the reactant. While taking concentration higher than the 125mg/ml the reducing agent will accommodate no free space for the reaction taking much time to complete the reaction and vice versa.

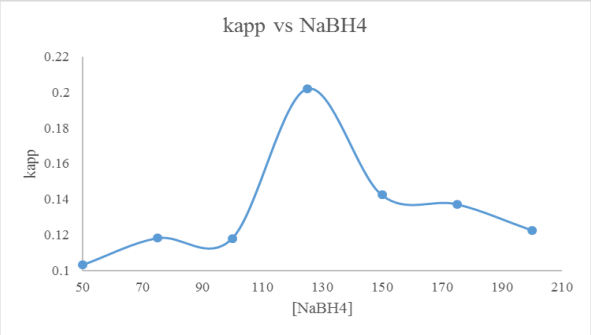

Fig. 4.9 Graph of $NaBH_4$ Reducing agent, k_{aap} vs time at various concentrations having Ag-pSty-pNipmam-Maa (CS) =0.2916 mg/mL and 0.086mM $NaBH_4$ at 34°C.

Figure 4.9 presents the deviation of the peaks which shows that the degradation changes by changing the concentration of the $NaBH_4$ and shows the maximum value at 125mg/ml for the required constant amount of MB. However, the degradation rate decreases after 125mg/ml because the dye is in constant quantity which shows the maximum degradation at 125mg/ml and does not give rise to any chance of further degradation.

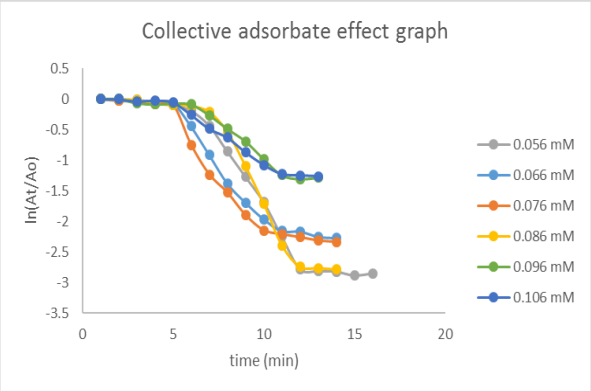

Fig. 4.10 Showing the effect of substrate (MB) on the reaction.

Effect of Substrate (MB)

Fig 4.10 shows a collective graph having different concentrations of substrate i.e. 0.056mM, 0.066mM, 0.076mM, 0.086mM, 0.096, and 0.106mM. At concentration (0.086mM) shows the best result. Substrate is material on which surface is to react. Here a substrate is Methylene blue on which surface reducing process has taken place using a reducing agent named Sodium Borohydride ($NaBH_4$). This suggests that at the start that is the initiation time there is no adjustment for the degradation of time due because at this time the dyes actually display the introduction of the dye. At the last of the graph there is still the same trend because at this time the degradation is completed. There is no longer any orientation towards the interaction of dyes with a reducing agent.

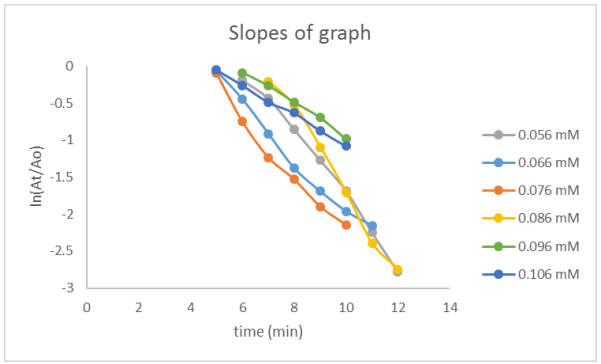

Fig. 4.11 Slope graph of MB-dye substrate.

In the decreasing peaks shown in the graph above, the reaction of the dye degradation in the presence of the reducing agent indicates that the degradation occurs at a fast rate while the reaction is continuing but after certain duration of time degradation has been completed. The lines listed above are different due to different concentration of MB, which indicates the maximum degradation at 0.086mM.

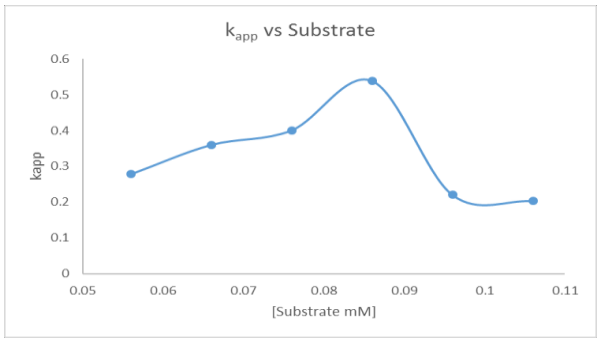

Fig. 4.12 Graph of substarte, kaap vs time at various concentrations having Ag-pSty-pNipmam-Maa (CS)=0.2916 mg/mL and 125mg/ml $NaBH_4$ at 34°C.

Figure 4.12 shows the divergence of the peaks showing that the degradation varies by varying the concentration of the dye, which increases by increasing the concentration of the dye. Then the maximum degradation at 0.086 mM at this catalyst and the reducing agent indicate the maximum degradation. But the rate of degradation falls since the particular concentration of the catalyte allows the interaction with the catalyst by increasing the concentration of MB. There is no room for the catalyst to connect with the dye and then continue to decrease rather than increase.

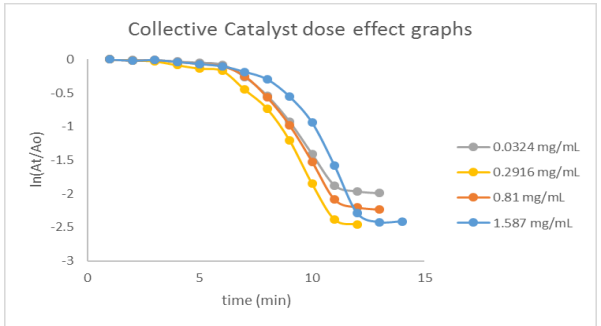

Fig. 4.13 Effect of Ag-pSty-pNipmam-Maa (CS) Catalyst.

Effect of Adsorbent

This demonstrates that at the start that is the induction time, there is no adjustment for the degradation of time, because at this time span, the dyes clearly display the introduction of the adsorbent. After this the beginning of the slope, which indicates that there is a rapid rate of degradation of the Eosin (y) with the passage of time. The same phenomenon is also seen in the final graph since the degradation is finished at this point. There is no more orientation to overlap the dyes with the catalyst that indicates the completion of the reaction. Catalyst dose effects were evaluated by maintaining a steady concentration of MB-dye and $NaBH_4$ at ambient temperature at the value of the apparent rate constants for the reduction of MB. In Figure ln(At /Ao) vs time. ln(At /Ao) linear plot region vs time to minimize MB from various hybrid dose microgels. Apparently, the constant rate increases linearly as the catalytic dose increases (Figure 4.13). The usable surface for the adsorption of reactive molecules increases as the dose of the catalyst is raised, resulting in an increase in the rate of reduction of MB. The reduction of MB does not start immediately.

The value of ln (At / Ao) is defined as the time of induction for a constant time.

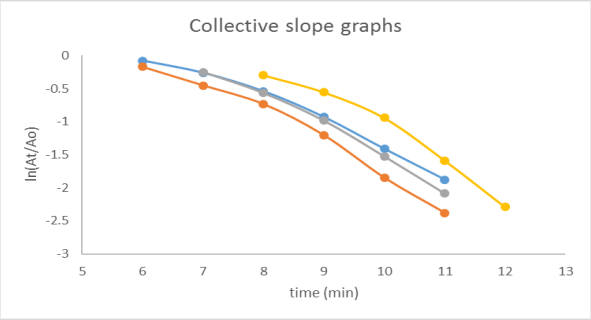

Fig. 4.14 Collective slope graph.

The reaction of degradation of the dye in the presence of the catalyst, which catalysis the reaction, shown in the diagram above, that degradation occurs at the speed of reaction and after a certain amount of time degradation is complete. Above graph represents the slope of ln(At/Ao) vs time.

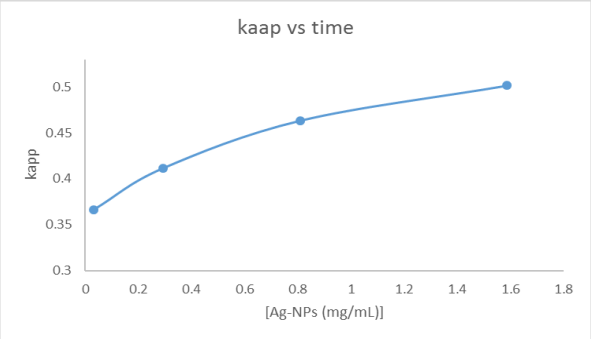

Fig. 4.16 Graph of Ag-pSty-pNipmam-Maa(CS) kaap vs time at various concentrations having 0.086 mM MB and 125mg/ml $NaBH_4$ at 34°C.

In the chart mentioned above, the reduction agent $NaBH_4$ demonstrates linearity between two variables, which is between kapp chart vs pSty-pNipmam-Maa (CS). The reduction agent's concentration increases with kapp. This effect is due to increase in active sites for the MB-dye substrate entering. Some time passed peak is matching parallel to x-axis because active sites of MB-dye is totally linked. If concentration of catalyst is increased then $NaBH_4$ and MB are absorbed on the surface of catalyst. Because active sites of catalyst increases with increase in concentration.

Conclusion

The discussion shows that pSty-pNipmam-Maa core shell microgels serve as active carrier of the Ag Nanoparticles. UV visible and FTIR analytical data confirmed the loading of spherical Ag nanoparticles with an average diameter of 10-12 nm in thin layer of core-shell microgels. At optimum condition the degradation of methylene blue using Ag-pSty-pNipmam-Maa with $NaBH_4$ was checked. The graph shows the reaction up to 13 minutes. The reaction was going on until 11th minute and becomes linear at 12th minute means reaction is completed. While in the absence of catalyst pSty-pNipmam-Maa the reaction was completed in 120 minutes indicating the efficiency of our catalyst against Methylene blue dye. This expresses the long lasting stability as well as superior catalytic-activity of our system.

Acknowledgement

I am very thankful to Mr. Habib Ullah student of Lahore Garrison University, DHA Phase 6, Sector C, Lahore, 54000, Punjab, Pakistan for arranging and composing the article for publication.

References

Ajmal, M., Farooqi, Z. H., Siddiq, M. (2013). Silver nanoparticles containing hybrid polymer microgels with tunable surface plasmon resonance and catalytic activity. *Korean Journal of Chemical Engineering, **30***(11), 2030-2036.

Atwater, H. A. (2007). The promise of plasmonics. *Sci. Am, **296***(4), 56-62.

Barnes, W. L., Dereux, A., Ebbesen, T. W. (2003). Surface plasmon subwavelength optics. *nature, **424***(6950), 824.

Brongersma, M. L, Shalaev, V. M. (2010). The case for plasmonics. *science, **328***(5977), 440-441.

Choi, M., Shin, K.-H., Jang, J. (2010). Plasmonic photocatalytic system using silver chloride/silver nanostructures under visible light. *Journal of Colloid and Interface Science, **341***(1), 83-87. doi:https://doi.org/10.1016/j.jcis.2009.09.037

J.E. Mark, C. Y. J., M.Y. Tang (1984). Simultaneous Curing and Filling of Elastomers. *Macromol-ecules, **17***(12), 2613-2616.

Kazancioglu, E. O., Aydin, M., Arsu, N. (2021). Photochemical synthesis of nanocomposite thin films containing silver and gold nanoparticles with 2-thioxanthone thioacetic acid-dioxide and their role in photocatalytic degradation of methylene blue. *Surfaces and Interfaces, 22*, 100793. doi: https://doi.org/10.1016/j.surfin.2020.100793

Odom, T. W., Schatz, G. C. (2011). Introduction to plasmonics: ACS Publications.

Paul, D. R., Robeson, L. M. (2008). Polymer nanotechnology: nanocomposites. *Polymer, **49***(15), 3187-3204.

Pradhan, N., Pal, A., Pal, T. (2002). Silver nanoparticle catalyzed reduction of aromatic nitro compounds. *Colloids and Surfaces A: Physicochemical and Engineering Aspects, **196***(2-3), 247-257.

Singh, H. P., Gupta, N., Sharma, S. K., Sharma, R. K. (2013). Synthesis of bimetallic Pt–Cu nanoparticles and their application in the reduction of rhodamine B. *Colloids and Surfaces A: Physicochemical and Engineering Aspects, **416***, 43-50.

Wen, J., Wilkes, G.L. (1996). Organic/inorganic hybrid network materials by the sol-gel approach. *Chemistry of Materials, **8***(8), 1667-1681.

Zhu, D., Wang, F., Gao, C., Xu, Z. (2008). Construction of PS/PNIPAM core-shell particles and hollow spheres by using hydrophobic interaction and thermosensitive phase separation. *Frontiers of Chemical Engineering in China, **2***(3), 253-256.